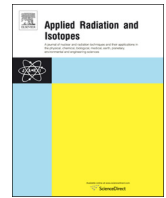




ELSEVIER

Contents lists available at ScienceDirect

## Applied Radiation and Isotopes

journal homepage: [www.elsevier.com/locate/apradiso](http://www.elsevier.com/locate/apradiso)

# Determination of radiocesium depth profile by unfolding method with imaging plate

Thanh Tat Nguyen, Tsuyoshi Kajimoto, Kenichi Tanaka, Satoru Endo\*

Quantum Energy Applications, Graduate School of Engineering, Hiroshima University, 1-4-1 Kagamiyama, Higashi-Hiroshima, Hiroshima 739-8527, Japan



## HIGHLIGHTS

- The radiocesium depth profile was derived from the readout intensity distribution of an imaging plate.
- The readout was unfolded with a response matrix for detected and source positions of radiation.
- The depth profiles were obtained with a 1 mm depth bin width.

## ARTICLE INFO

### Keywords:

Depth profile  
Imaging plate  
Response function  
Unfolding method  
Depth bin (4–6 keywords)

## ABSTRACT

Radiocesium depth profiles in Fukushima soil cores were derived with an unfolding method by using an imaging plate with a response matrix for  $^{134}\text{Cs}$ ,  $^{137}\text{Cs}$ , and  $^{40}\text{K}$  radionuclides calculated by a PHITS simulation. The unfolded depth profiles were validated by comparison with profiles measured with a Ge detector. The unfolded depth profiles agreed well with those measured by the Ge detector. The depth profiles obtained were obtained with a 1 mm depth bin width and are useful for estimating the migration of radiocesium in soil.

## 1. Introduction

The Great East Japan Earthquake and tsunami in March 2011 caused the Fukushima Daiichi nuclear power plant (FDNPP) disaster. A large amount of radionuclides was released into the air, and then deposited on the ground surface (Endo et al., 2013). Short-lived radionuclides, such as  $^{132}\text{I}$ ,  $^{132}\text{Te}$ ,  $^{129}\text{Te}$ ,  $^{129\text{m}}\text{Te}$ ,  $^{131}\text{I}$ , and  $^{136}\text{Cs}$ , decayed to undetectable levels within a year. However,  $^{134}\text{Cs}$  and  $^{137}\text{Cs}$  (radiocesium) with half-lives of 2.06 and 30.2 years, respectively, take a long time to decay. Thus, radiocesium in soil will cause internal and external exposure in humans and the environment for a long time after the accident. Information about radiocesium in the soil is useful for estimating the air dose from contaminated ground and root uptake by plants. Based on this information, we also clarify the characteristics of radiocesium dynamics in soil. The migration velocity and diffusion coefficient are migration indexes for radiocesium in soil, and are determined by fitting the radiocesium depth profile (Arapis et al., 1997; Szerbin et al., 1999; Krstic et al., 2004; Almegren and Isaksson, 2006). The depth profile has been obtained by measuring the activity of radiocesium in thin layers separated from a soil core. Generally, the depth bin width for this technique is several centimeters.

For uncultivated upland field soil contaminated by the FDNPP

accident, Shiozawa (2013) reported that the migration velocity of radiocesium was 4–7 mm per month during the first 3–4 months after the accident, and 0.4–1.4 mm/y 1 year after the accident. They also predicted that the migration velocity would decrease with time. Takahashi et al. (2015) estimated the relaxation depth of radiocesium (mean migration depth) for different types of land in contaminated areas of Fukushima Prefecture. The results suggested the migration velocity was small 4–21 months after the accident. They reported migration velocities of 1.6 mm/y in meadow land, 3.7 mm/y in farmland, 1.2 mm/y in tobacco fields, and 10.1 mm/y in paddy fields. Based on these results, radiocesium migrates several millimeters to 1 cm in soil over several years, except for in paddy field soil. To analyze radiocesium migration precisely, the depth bin width should be reduced to several millimeters. However, it is difficult to cut thinner layers from soil cores.

In this paper, we propose a method that uses an imaging plate (IP) and Bayesian unfolding analysis to determine the depth profile with a millimeter depth bin width. The proposed method is based on unfolding the IP intensity profile of an IP with a response matrix for detected and source positions of radiation from each radionuclide ( $^{134}\text{Cs}$ ,  $^{137}\text{Cs}$ , and  $^{40}\text{K}$ ) of a soil core. The method is validated by applying it to different types of IP intensity profiles and the obtained results are compared with

\* Corresponding author.

E-mail address: [endos@hiroshima-u.ac.jp](mailto:endos@hiroshima-u.ac.jp) (S. Endo).

<https://doi.org/10.1016/j.apradiso.2018.09.014>

Received 2 October 2017; Received in revised form 6 May 2018; Accepted 12 September 2018

Available online 13 September 2018

0969-8043/© 2018 Elsevier Ltd. All rights reserved.

**Table 1**  
Position and dose rate at a height of 1 m from the ground for the samples.

Location	Global positioning system		Dose rate ( $\mu\text{Sv/h}$ )
	Latitude	Longitude	
Nagadoro Jumonji 2013	37.61281	140.7494	5.6
Komiya Magata 2013	37.6620	140.7746	0.8
Nagadoro Magata 2013	37.60396	140.7779	9.5
Nagadoro Jumonji 2015	37.61281	140.7494	4.1

those measured by a low-background Ge detector.

**2. Material and methods**

**2.1. Soil sampling**

Iitate village, which is 30–45 km north-northwest of FDNPP, was heavily contaminated by the radioactive materials released during the FDNPP disaster (Imanaka et al., 2012). Since 2011, our team has monitored the air dose rate and collected about 10 soil cores (30 cm deep, 5 cm in diameter), annually. The soil core sampling method in this investigation is a bore core sampling method which was popularly applied in previous researches (Almegren and Isaksson, 2006; Fujiwara et al., 2012). To validate the proposed method, four IP intensity profiles that are representative of the soil cores were selected. The soil types in these cores were determined based on the National Institute for Agro-Environmental Sciences guidelines (NIAES, 2001) as a medium coarse grain gray soil (Nagadoro Jumonji) and a gray lowland soil (Nagadoro Magata). A soil core was taken from a decontaminated field (Komiya Magata) after decontamination work had scraped 5 cm of surface soil away and the field was covered with uncontaminated granite soil. The depth profile of this core is different from those of undisturbed soils collected at Nagadoro Jumonji and Nagadoro Magata. The depth profiles are described in Subsection 3.1. The sampling positions and dose rate 1 m from the ground at the time of sampling are listed in Table 1.

**2.2. Measurement of IP intensity profiles**

The soil cores were wrapped in an IP (BAS-IP MS 2040, Fuji film Co., Ltd.; 20 × 40 cm) and exposed in a lead chamber for 1 day. Two-dimensional images were read by an image analyzer (Typhoon FLA 7000, GE Healthcare Life Science Co.). Depth profiles of the average IP intensity and standard deviation ( $\sigma$ ) were obtained at 0.5 mm depth steps (0–30 cm, 600 depth bins) from the two-dimensional imaging by Image Quant TL software (GE Healthcare Life Science Co.). The IP intensity profiles were used for unfolding analysis.

**2.3. Radioactivity measurements of radiocesium and <sup>40</sup>K in soil cores**

After the IP measurement, the soil cores were divided into seven

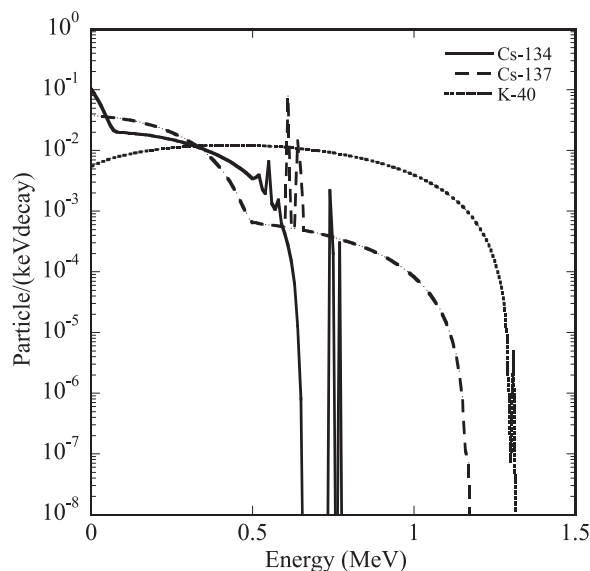


**Fig. 2.**  $\beta$ -ray source term for <sup>134</sup>Cs (blue), <sup>137</sup>Cs (red), and <sup>40</sup>K (black). (For interpretation of the references to color in this figure legend, the reader is referred to the web version of this article.)

layers from the surface to a depth of 30 cm: two 2.5-cm-thick layers in the high-intensity IP region and five 5-cm-thick layers in the remaining region. The samples were dried at 80 °C for 17–24 h, and sieved with a 2 mm mesh to remove gravel and plant roots. The soil layer was placed in a U-9 container and set on the endcap of a low-background Ge detector (GMX-30200-P, ORTEC). The detection efficiencies for the full-energy  $\gamma$ -ray peaks of 605, 662, and 1461 keV emitted from <sup>134</sup>Cs, <sup>137</sup>Cs, and <sup>40</sup>K, respectively, were determined from the detection efficiency curve obtained by measuring  $\gamma$ -rays from <sup>109</sup>Cd, <sup>57</sup>Co, <sup>139</sup>Ce, <sup>51</sup>Cr, <sup>85</sup>Sr, <sup>137</sup>Cs, <sup>54</sup>Mn, <sup>88</sup>Y, and <sup>60</sup>Co in standard volume sources (MX-033, Japan Isotope Association). The detection efficiency of the Ge detector was determined with statistical error of less than 1% and systematic uncertainty of less than 5% (Endo et al., 2013). The correction factor of the detection efficiency for cascade summing events at 605 keV for <sup>134</sup>Cs was estimated to be 1.15 by Kajimoto et al. (2015), and was corrected for determining <sup>134</sup>Cs radioactivity.

**2.4. Response function calculated by PHITS**

The response function was defined as the energy deposition profile,  $E(d; x)$  [MeV/Bq], in the IP sensitive layer as a function of depth  $d$  from thin radionuclide sources of <sup>134</sup>Cs, <sup>137</sup>Cs, and <sup>40</sup>K at depth  $x$ , and was calculated with PHITS code (Sato et al., 2013). The energy depositions were calculated separately for  $\gamma$ -rays and  $\beta$ -rays for the <sup>134</sup>Cs, <sup>137</sup>Cs, and <sup>40</sup>K sources. The geometry for the PHITS calculation consisted of an IP and a 257- $\mu\text{m}$ -thick polyvinyl chloride tube enclosing the soil core with

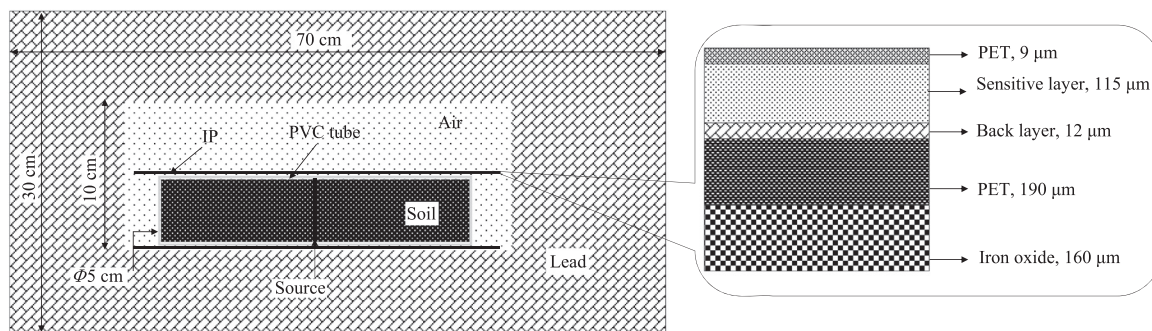


**Fig. 1.** Schematic of PHITS calculation geometry.

Download English Version:

<https://daneshyari.com/en/article/11026279>

Download Persian Version:

<https://daneshyari.com/article/11026279>

[Daneshyari.com](https://daneshyari.com)